

Combining cues in contour orientation discrimination

Ariella V. Popple *, Dennis M. Levi

School of Optometry, Minor Hall, University of California at Berkeley, Berkeley, CA 94720-2020, United States

Received 17 October 2003; received in revised form 24 March 2004

Abstract

The perceived orientation of a Gabor-patch contour is determined, in part, by shifts in carrier phase between the patches [Popple, A. V. & Sagi, D., 2000. A Fraser illusion without local cues? *Vision Research*, 40, 873–878; Popple, A. V. & Levi, D. M., 2000a. A new illusion demonstrates long-range processing. *Vision Research*, 40, 2545–2549; Popple, A. V. & Levi, D. M., 2000b. Amblyopes see true alignment where normal observers see illusory tilt. *Proceedings of the National Academy of Sciences of the United States of America*, 97, 11667–11672]. Here we show that perceived orientation results from the combination of at least three stimulus cues: (1) patch orientation, (2) contour envelope orientation, and (3) between-patches orientation, which is a function of phase-shifts. In a series of three experiments, we investigated how these three cues were combined. The data are consistent with weighted cue combination.

© 2004 Elsevier Ltd. All rights reserved.

Keywords: Gabor patch; Contour; Phase; Cue combination; Fraser illusion

1. Introduction

The perceived orientation of a single circular Gabor patch, an oriented sinusoidal carrier modulated by a symmetric Gaussian contrast envelope, is given by the orientation of the carrier. However, when a stimulus is composed of two or more such patches, there are many different possible cues to the orientation of the composite stimulus, in addition to the first-order carrier orientation inside each patch. One cue is the orientation of the composite second-order contrast envelope. When the centroids of the individual patches are aligned in a row, this cue falls along their axis. Slight misalignments of the carriers between the patches, such as those caused by shifting their phase, give a further cue to orientation. To summarize, given two circular Gabor patches, or a contour of such patches, there are three cues to their orientation that can be manipulated independently. These

cues are: (1) the carrier orientation of each patch; (2) the orientation of the contour envelope; and (3) the phase-shift between the patches.

One might argue that the orientation of the contour, which is objectively a set of patches grouped together, is equal to the orientation of their collective second-order contrast envelope. However, it is well known that human observers, even when asked to ignore first-order cues, are not able to do so. One example is Fraser's twisted cords illusion, in which an elongated envelope appears to be tilted in the same direction as the black and white carrier bars inside (Fraser, 1908; Fig. 1c). Another example is the phase-shift illusion, where a horizontal row of horizontal patches appears tilted, only because their carriers are shifted in phase (Popple & Levi, 2000a, 2000b; Popple & Sagi, 2000; Fig. 1a). One possible reason for this discrepancy between the objectively defined orientation, and human perception of it, is that in the natural visual environment first-order cues to contour orientation arising from luminance and hue are more commonplace and reliable than second-order cues. Field, Hayes, and Hess (1993) showed that Gabor

* Corresponding author. Tel.: +1 510 643 8685; fax: +1 510 643 8733.

E-mail address: ariellap@berkeley.edu (A.V. Popple).

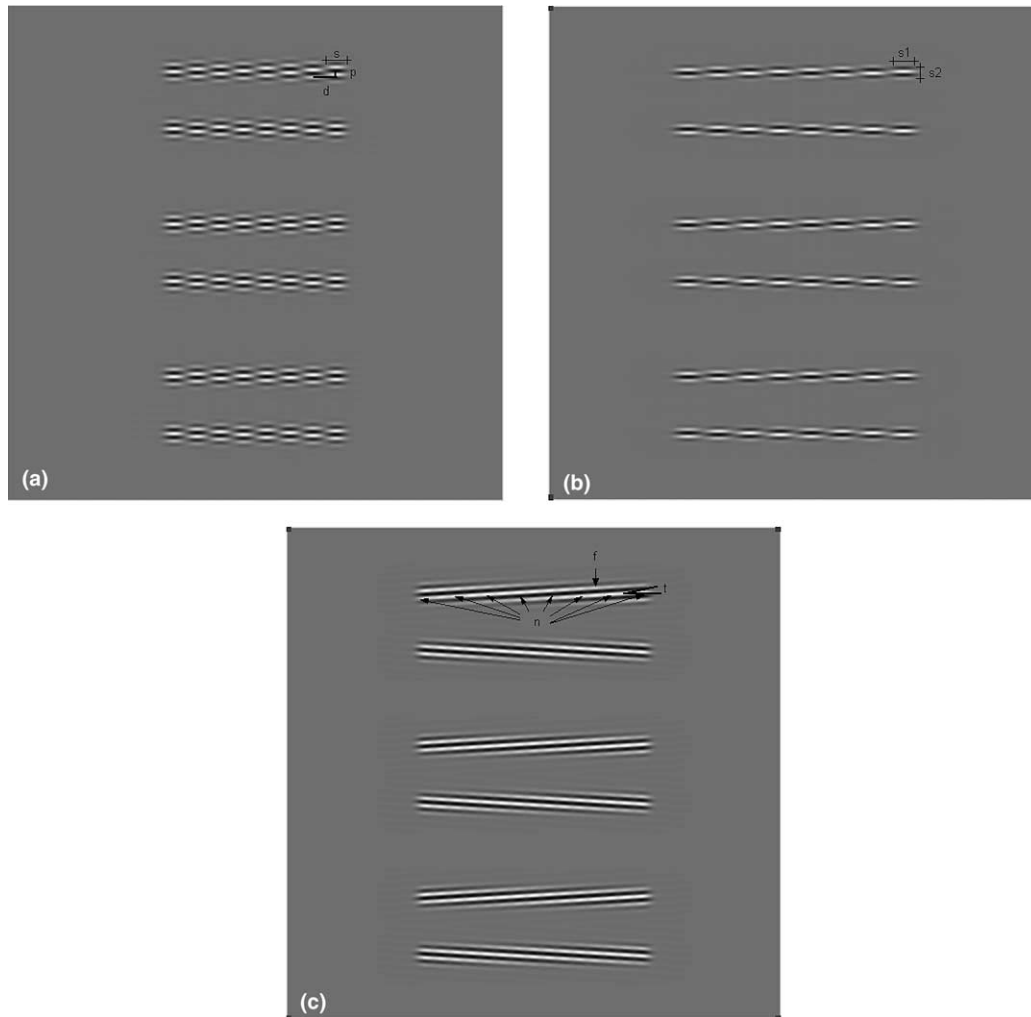


Fig. 1. Sample stimuli and experimental design. (a) In experiment 1, we varied the phase-shift (p) and displacement (d) between the patches, as well as their size (s). This example shows $p = 135^\circ$ phase angle, $d = 3\lambda$, and $s, \sigma = 0.75\lambda$, where λ is the carrier period, and σ is the standard deviation of the patch envelope. (b) In experiment 2, we varied the shape of the patches, by changing their size along and across the row ($s1$ and $s2$, respectively). Phase-shift, p , was fixed at 90° phase angle, and displacement, d , at 4λ . This example shows $s1 = \lambda$ and $s2 = \lambda/2$. (c) In experiment 3, we varied the number (n) of patches in the row, their tilt (t), and whether or not the spaces between them were filled (f). This example shows $n = 8$, in the 'filled' condition (see text for details). As in experiment 2, the phase-shift, p , was fixed at 90° phase angle, and displacement, d , at 4λ .

patches oriented along the same curve group together to form a contour much more readily than a group of patches that merely share the same orientation. In other words, the contour is seen more easily when its local orientation is the same as that of its constituent patches. Second-order cues are useful for breaking camouflage, only if first-order cues are insufficient.

The visual cortex contains many different kinds of neurons sensitive to orientation. In primary visual cortex (V1), simple cells respond only to black and white bars of a particular orientation and contrast polarity, whereas complex cells respond to orientation regardless of polarity. Some cells in V1, and many in V2, respond also to second-order boundaries and illusory contours (Mareschal & Baker, 1998; Nothdurft, Gallant, & Van Essen, 1999; Peterhans & von der Heydt, 1993). When the observer is asked to make a judgment about contour

orientation, how are these different sources of information, both in the stimulus and in the visual system, combined? Ideally, when observers are told to base their decision on one particular cue, they should ignore the other cues. However, if the natural visual environment provides independent orientation cues that are more often coincident than conflicting, then combining the cues using Bayes' rule, weighting them by their inverse variance, should improve the precision with which object orientation can be determined (see Appendix A for derivation and assumptions). Such cue combination could become hard-wired, making it possible that observers will no longer have access to the original cues. Instead, information may be remapped onto a space where the contour has a unique global orientation that confounds second-order and first-order cues, and the residual information is used to determine its local surface texture. We

investigated psychophysically how these cues are combined to determine the perceived global orientation of Gabor-patch contours, specifically rows of identical patches.

2. Methods

2.1. Observers

Nine observers participated in experiment 1, and three in experiments 2–3 (a fourth observer was rejected because her thresholds were very variable, although perceived orientation was similar to other observers). All observers had normal or corrected to normal visual acuity. All except AP and SL were naïve as to the purpose of the experiments.

2.2. Apparatus and stimuli

Stimuli were textures of 3 cpd Gabor patches arranged in three identical pairs of rows. The two rows in each pair were mirror images of each other, tilted in opposite directions, to make the row-pairs taper left or right. Stimuli were generated by a VSG 2/3 card mounted on a Komputer PC, and displayed for 110 ms on a gamma-corrected monitor at mean luminance 40 cd/m². Sample stimuli are shown in Fig. 1. Stimuli were shown at the maximum contrast available. This means that separated patches were at 100% contrast (e.g. Fig. 1a and b), whereas dense patches were at 50% (e.g. Fig. 1c). See Popple and Levi (2000a) for more comprehensive details.

2.3. Design

In each experiment, we systematically varied two or more properties of the stimulus contour rows (see Fig. 1 for details). For clarity, design details of each experiment precede the relevant results section. The dependent variable was the perceived orientation of the rows. The observer judged whether the row-pairs tapered left or right.

2.4. Procedure

The perceived tilt of the rows away from horizontal was nulled by rotating each row in the opposite direction to its perceived tilt. Each row was rotated as a whole object, including both the first-order carrier and the second-order envelope, such that the orientation and position of the black and white carrier bars relative to their surrounding contrast envelope did not change, only the orientation of this whole-row object in the stimulus plane on the monitor surface was varied. Using the method of constant stimuli, there were 20 repetitions of

13 angles in each block. The direction of the phase-shifts in each row (up or down) was randomized between trials, making the row-pairs appear to taper left or right. The frequency of responses in the direction of the phase-shifts was recorded at each angle of rotation. Data were fitted in Matlab with cumulative normal functions using Probit weighting (Finney, 1971). The finger error rate (kept constant within observers and experiments) was never greater than 5%. The mean of the fitted cumulative normal is a measure of the perceived orientation. Its standard deviation is a measure of the orientation discrimination threshold. Each observer's data were fitted simultaneously within each experiment, pooling together similar conditions to estimate thresholds. All error bars from this and subsequent model fits show 95% confidence intervals computed using Matlab.

3. Results

3.1. Experiment 1

In experiment 1 we varied the phase-shift (p) and the displacement (d) between the Gabor patches, and the size (s) of the Gabor patches so that they could be packed closer together without overlapping (see Fig. 1a). Perceived orientation peaked close to 90° phase-shift, for displacements of 3λ or more, and slightly lower for 2λ (Fig. 2a). Data were fitted with a 2-line fit anchored at (0,0) and (180,0) to confirm this observation. The amplitude of the peak decreased monotonically with increasing displacement. Fig. 2b shows the means across observers, with error bars indicating that the standard deviations between observers were small compared with the size of the effect, at least for separations up to 4λ . The estimated mean peak phase-shift across observers is plotted in Fig. 2c. The large error bars at 5λ are likely due to the small size of the effect at this separation. Where the amplitude is close to zero, it can be hard to find the peak. Orientation thresholds rose slightly with increasing phase-shift (grey bars in Fig. 2a).

3.2. Experiment 2

Patch size is an important determinant of the amplitude of the peak (Fig. 2b). This effect of patch size may have been the result of increasing either patch elongation in the rows, or the number of visible cycles in each patch. In experiment 2 we varied the shape of the patches as well as their size, by changing the horizontal and vertical space constants of the patches (s_1 and s_2) independently (see Fig. 1b). We found that increasing elongation (horizontal size) both increased perceived orientation, and reduced thresholds (Fig. 3). Although these effects are strongest in AP, similar trends can be

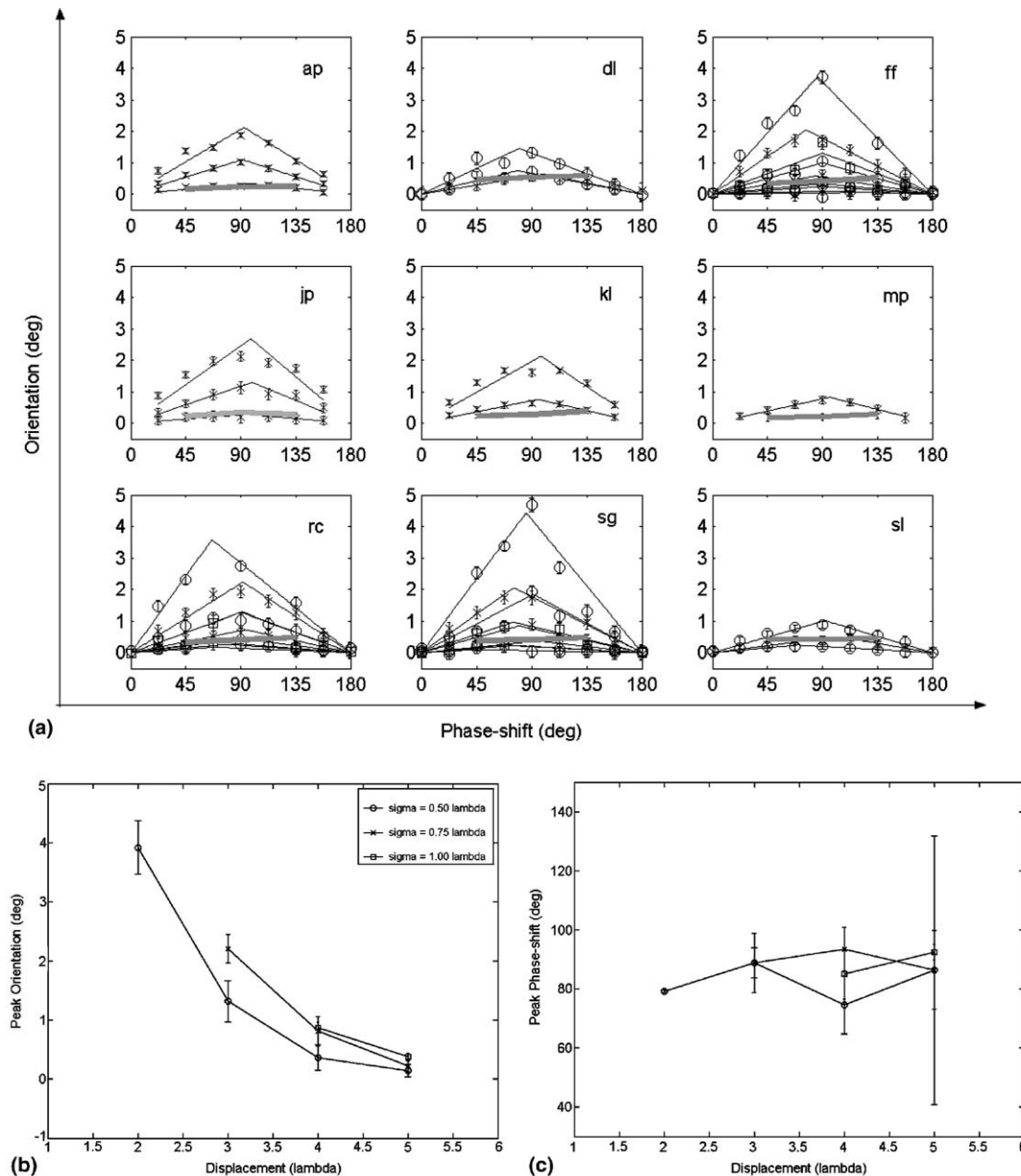


Fig. 2. Experiment 1 results. (a) Perceived orientation varied by phase-shift and displacement, peaking at 90° phase angle, and decreasing with increased displacement. Different symbols indicate different patch sizes—see legend. Grey bars indicate orientation threshold, fitted across similar conditions. Series in (a) were fitted using a 2-line fit. (b) The amplitudes of these peaks decreased with increasing displacement, and also increased with increasing patch size. (c) The peaks were found to be near 90°. (b) and (c) show means across observers, with error bars indicating standard deviations across observers.

seen in all three observers, particularly in the larger interval between 0.5λ and 1.0λ. Increasing the number of visible cycles within the patches (vertical size) made no consistent difference to perceived orientation, or thresholds.

3.3. Experiment 3

The Fraser illusion uses elongated patches. In experiment 3 we tried to relate the phase-shift illusion to the Fraser illusion. There are two features that distinguish

the two illusions. First, in the phase-shift illusion the patches are co-aligned with the row. Second, there are gaps between them. In this experiment, we compared the phase-shift illusion ('phase-shift' condition) with a Fraser illusion formed by a tilted grating sampled at the same frequency along the row as the phase-shift illusion ('tilted' condition), or sampled at double the frequency ('filled' condition). In another control condition, the phase-shifted patches were tilted in the opposite direction ('opposite-tilt' condition, not shown). This is similar to the tilted-chain illusion we described in

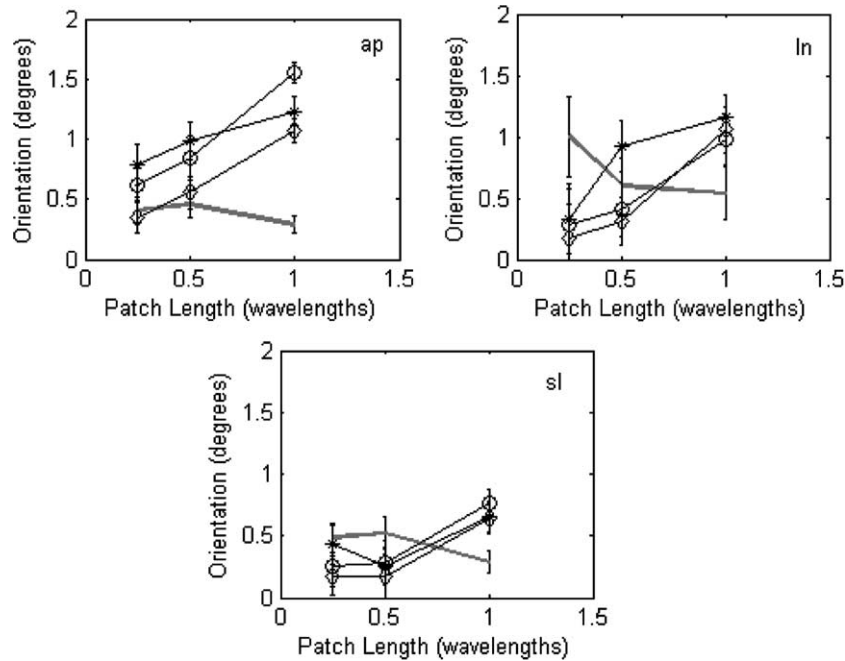


Fig. 3. Experiment 2 results. Perceived orientation increased with increasing patch elongation (sl) along the row, but did not vary consistently with patch width across the row. Different symbols indicate patch width (s2). Thresholds (grey lines), fitted over the different widths, were lower for longer patches.

Popple and Levi (2000b). We varied the number of patches (n), their tilt (t), and whether the gaps between them were filled (f). For a sample of the ‘filled’ condition, see Fig. 1c.

We found that the data were well described as an exponential function of the number of patches anchored at the local orientation of a single patch (Fig. 4a). When this data were fitted with a cumulative normal curve having a spread and an asymptote, the spreads indicated an integration length of 3–5 patches and did not vary consistently or significantly between conditions (circles, Fig. 4b). The asymptotic perceived orientation varied by condition, and for the phase-shift condition was intermediate between the tilted/filled and opposite-tilt conditions (circles, Fig. 4c). Thresholds also decreased steadily as the number of patches increased (Fig. 4d), with an asymptote at about 0.5° , based on an exponential fit anchored at a single-patch threshold of 1° (from the literature). This asymptote did not vary much with condition, but was slightly higher in the ‘opposite-tilt’ condition than in the ‘phase-shift’ condition, consistent with the results of experiment 1 (asterisks, Fig. 4c). As with perceived orientation, the spread of the fitted function, indicating integration length, was about 3–5 patches and did not vary much between conditions (asterisks, Fig. 4c).

If the visual system combines the three orientation cues we identified in the Introduction according to Bayes theorem, we can derive expressions for sensitivity and perceived orientation (see Appendix A for derivation and assumptions).

$$\frac{1}{\sigma^2} \approx \frac{1}{\sigma_E^2} + \frac{1}{\sigma_P^2} + \frac{1}{\sigma_B^2} \quad (1)$$

$$\frac{\theta}{\sigma^2} \approx \frac{\theta_E}{\sigma_E^2} + \frac{\theta_P}{\sigma_P^2} + \frac{\theta_B}{\sigma_B^2} \quad (2)$$

In this scheme, σ_E is the contour envelope orientation threshold, σ_P the single-patch orientation threshold, σ_B the between-patch threshold of orientation discrimination based on phase-shift, and σ the combined orientation threshold. Additionally, θ_E is the contour envelope orientation, θ_P the single-patch orientation, θ_B the between-patch orientation based on phase-shift, and θ the combined orientation. The above expressions are approximations because we ignore the variability due to the differences between the orientations given by the three cues, however the data suggest that such variability was small, since thresholds did not vary much by condition (Fig. 4c). Estimates of perceived orientation in each condition can be derived from (2), relative to the envelope orientation set at zero. In the phase-shift condition, patch orientation is zero, therefore:

$$\theta_{\text{phase}} \approx \sigma^2 \left(\frac{\theta_B}{\sigma_B^2} \right) \quad (3)$$

In the tilted and filled conditions,

$$\theta_{\text{tilt}} \approx \sigma^2 \left(\frac{\theta_B}{\sigma_B^2} + \frac{\theta_P}{\sigma_P^2} \right) \quad (4)$$

and in the opposite-tilt condition,

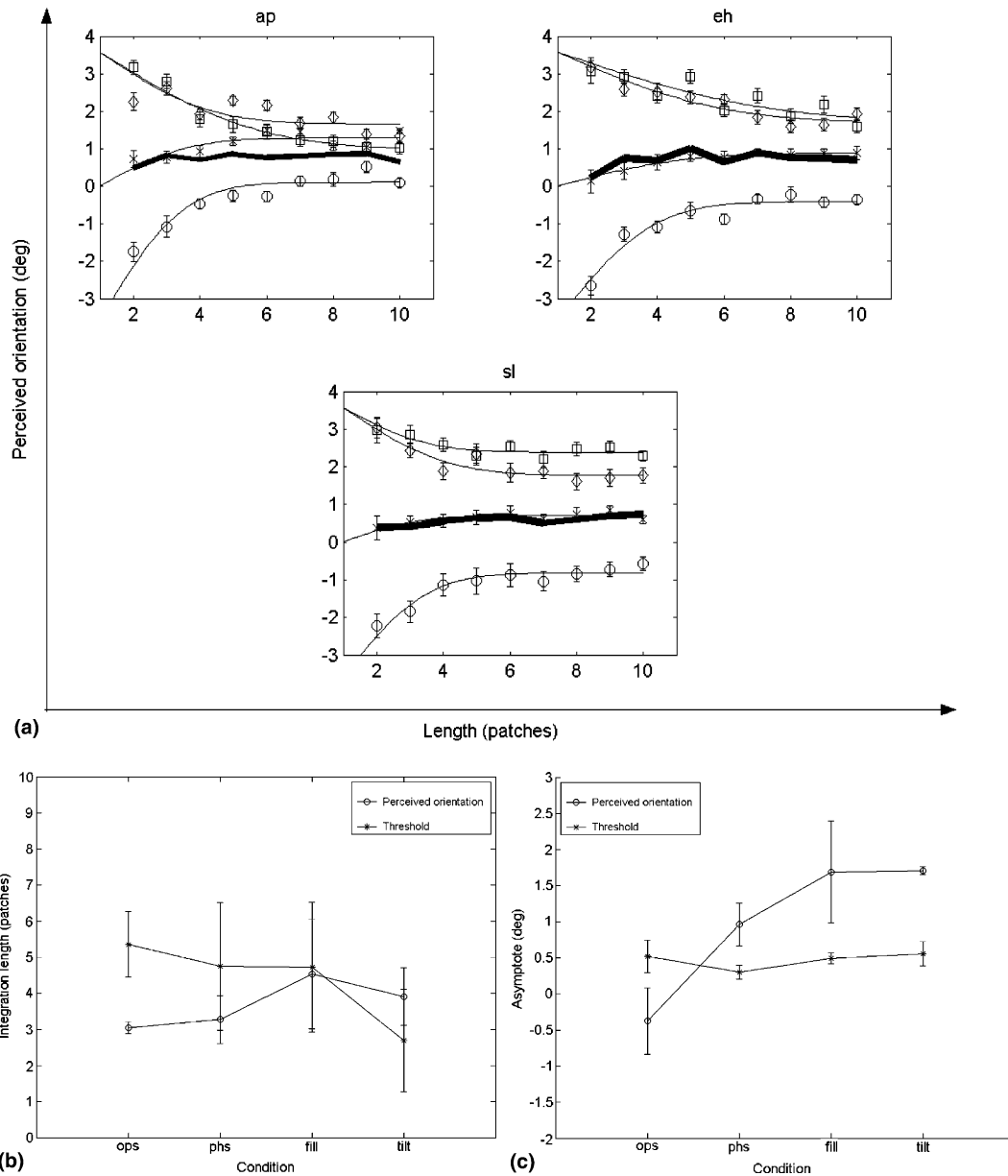


Fig. 4. Experiment 3 results. (a) Perceived orientation varied with the number of patches. Conditions are indicated by symbols: circles—opposite tilt, x's—phase-shift, squares—filled, diamonds—tilted (see text for details). Thick lines indicate model predictions for phase-shift, halfway between opposite-tilt and filled/tilted results. (b) The integration length of the fitted functions was 3–5 patches. Our model predicts that this should be the same for thresholds and perceived orientation. (c) Asymptotic perceived orientation was different for the different conditions (circles), although the asymptotes of the threshold were relatively independent of condition (asterisks). According to the model, perceived orientation in the phase-shift condition should be halfway between opposite tilt and filled/tilted (filled and tilted conditions should yield the same results). (b) and (c) show means and standard deviations between observers. (d) Thresholds generally decreased as the number of patches was increased.

$$\theta_{\text{ops}} \approx \sigma^2 \left(\frac{\theta_B}{\sigma_B^2} - \frac{\theta_P}{\sigma_P^2} \right) \quad (5)$$

From 3 to 5,

$$\theta_{\text{tilt}} - \theta_{\text{phase}} \approx \theta_{\text{phase}} - \theta_{\text{ops}} \approx \sigma^2 \left(\frac{\theta_P}{\sigma_P^2} \right) \quad (6)$$

Consistent with this formulation, perceived orientation in the phase-shift condition was halfway between the opposite-tilt and filled/tilted conditions, the latter two

being more-or-less equal (compare data (x's) with thick lines in Fig. 4a). Given the patch orientation of 3.5°, estimating the combined threshold from the data at about 0.5° at limit, and assuming a patch threshold of about 1°, Eq. (6) yields a difference between the conditions of about 1° perceived orientation, close to what we found (Fig. 4c). From the data and Eq. (3), the threshold for phase is about 1.3°, giving an envelope threshold from (1) of 0.6° at minimum.

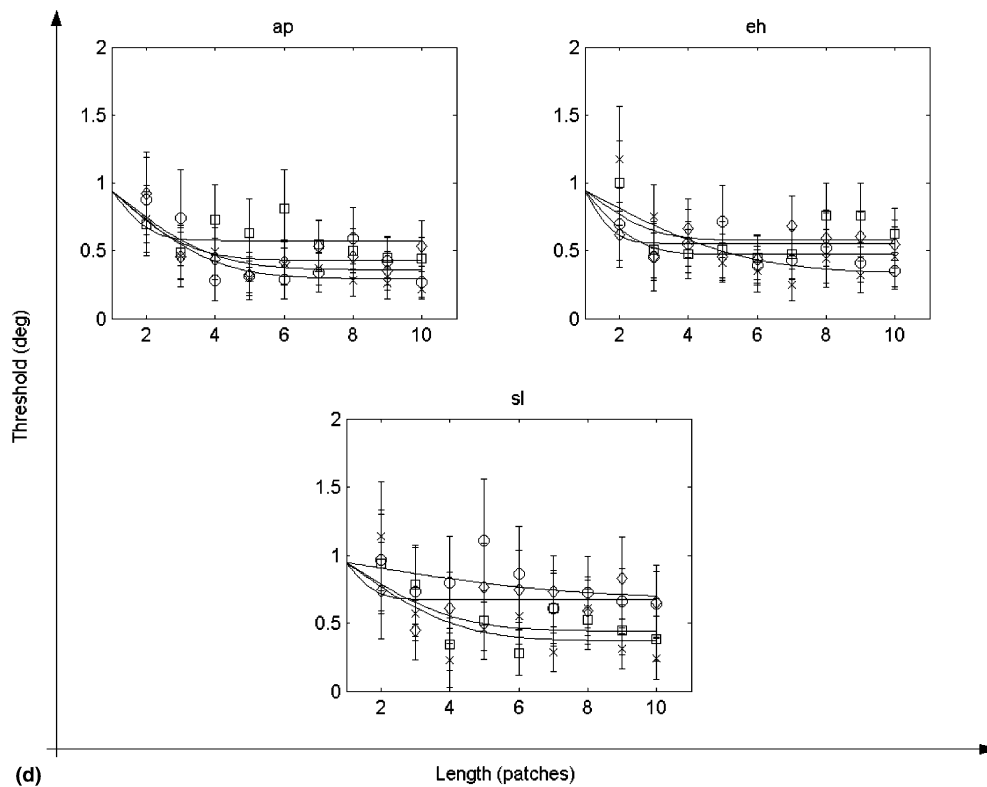


Fig. 4 (continued)

4. Discussion

The data suggest that, in judging the orientation of a Gabor-patch contour, the visual system forcibly combines the three orientation cues we identified: (1) envelope orientation; (2) patch orientation; and (3) between-patches orientation. The weighting of the cues is consistent with Bayes' theorem, however see [Appendix A](#) for underlying assumptions.

Experiment 1 shows that the between-patches cue can be broken down into Sine and Cosine components, with perceived orientation determined by the amount of Sine (maximal at 90° phase-shift), and thresholds influenced by the sign of the Cosine (most negative at 180° phase-shift). The magnitude of the orientation suggested by phase-shifts depends on the spacing between the patch centers. However, experiments 1 and 2 both show that the influence of this cue depends on the spacing between the edges of the patches, suggesting a local mechanism. Experiment 3 shows that the cues are integrated together over a number of patches.

Previous models have considered the influence of first-order orientation cues on second-order orientation perception in elongated Gabor patches similar to [Fig. 1c](#). Such models have generally been filter-rectify-filter models containing some nonlinearity in the way the filters are connected ([Dakin, Williams, & Hess, 1999](#); [Morgan & Baldassi, 1997](#); [Morgan, Mason, & Baldassi, 2000](#)). In

the past, we have also suggested linear filtering models ([Popple & Levi, 2000a, 2000b](#)). Without modification, these models cannot simulate the effects of phase-shift and row length we report here, nor can they simulate the effects of bandwidth described by [Skillen, Whitaker, Popple, and McGraw \(2002\)](#). We are now less ambitious in our modeling, preferring to examine how stimulus information sources might be combined by the visual system in reaching a sensory judgment, without prescribing a particular algorithm or physiological process.

A plausible reason for our results is a range limitation on the visual system's ability to integrate the envelope information from successive patches and estimate second-order orientation. Within this limited range ([Fig. 4b](#)) the second-order cue may be relatively weak compared with the combination of local orientation signals within and between the patches. [Fig. 4d](#) shows that adding more patches brings the threshold down by about 50%, suggesting that the envelope cue alone is only slightly better than the ~1° single-patch threshold, and can be estimated from our model at about 0.6° at minimum. Consistent with this limitation, patch elongation influenced thresholds, presumably by improving single-patch thresholds, even in a long row where row envelope information was saturated ([Fig. 3b](#)). This limited pooling range may be the reason why the global orientation estimate is never entirely based on the second-order orientation cue alone, when competing first-order information is

available. Within this global estimate, the between-patches cue seems to be weighted almost as much as the within-patches cue. The equality between high-contrast, visible patches and low contrast between-patch signals may be due to the contrast invariance of orientation tuning functions in V1 (Hansel & van Vreeswijk, 2002).

An interesting consequence of the model is that the increase in perceived orientation between two and four patches in the phase-shift condition implies that the weight given to the phase-shift cue must go up in this interval, because the orientation implied by the phase-shifts does not change. Perhaps this is due to an increase in sensitivity for phase-shift discrimination. Another possibility is that the phase-shift cue is more easily discarded by attention when there are only 2–3 patches, as suggested by the work of Akutsu and Levi (1998). We plan to test this using a different task.

It is important to emphasize that the simplistic application of Bayes' rule for combining relevant cues to the task of estimating contour orientation will not work here, as the first-order cues are not strictly speaking relevant in this task, and yet they influence performance. Previous work by us and others has indicated that independent visual cues are combined in a manner consistent with Bayes' rule in a number of different tasks, including estimating the orientation of an elongated patch (Skillen et al., 2002), contour curvature (Levi, Wing-Hong Li, & Klein, 2003), and surface slant (Hillis, Ernst, Banks, & Landy, 2002). Here, instead, we must consider an application of the rule that includes selected 'noise' variables, possibly dependent on the statistics of the natural visual environment.

Kersten and Schrater (2002) proposed that 'Pattern Inference Theory' be used to combine cues according to their relevance in naturalistic tasks, as well as their precision. Another approach is to couch the application of Bayes' rule in terms of remapping independent sensory cues onto the space of behaviorally relevant stimulus properties. For example, Hillis et al. (2002) found that, in practice, observers used perceived surface texture properties to discriminate between planes that could not be distinguished based on their perceived slant. Behaviorally, slant is relevant for understanding the layout of the environment, and surface texture is relevant for segmenting and recognizing objects. In our stimuli, contours have internal texture properties (local orientation and plaid-like appearance) as well as global orientation. These internal texture properties are relevant for understanding the 3D structure and topology of real contours, as hinted at by Fraser's original term for his illusion—twisted cords. Comparing Fig. 1a and c, as well as the difference in global tilt, their appearance is very different: Fig. 1a appears more plaid-like than Fig. 1c, and in Fig. 1c the local orientation appears more tilted compared with the global orientation. Perhaps the

visual system maps local phase and orientation, as well as envelope orientation, onto a space that represents object orientation and 3D surface properties, losing conscious access to the original cues. Our stimuli were brief (110 ms), and it is possible that, with longer stimulus intervals, observers may be able to disentangle such cues by using directed attention (Akutsu & Levi, 1998).

In conclusion, although observers are able to judge precisely the global orientation of a briefly presented Gabor-patch contour, this global estimate is inaccurate, insofar as it confounds first and second-order cues to orientation. First-order cues between the patches influence global orientation almost as much as first-order cues within the patches.

Acknowledgments

I would like to acknowledge RO1EY01728 from the National Eye Institute, NIH, to D. Levi.

Appendix A

The most frequently cited source for deriving cue combination from Bayes' theorem is Yuille and Bülthoff's (1995) chapter on Bayesian decision theory and psychophysics. Here is a summary and generalization of the arguments found mainly in their appendix:

According to Bayes,

$$P(S|I) = \frac{P(I|S)P(S)}{P(I)} \quad (\text{A.1})$$

where I is the image, and S is the stimulus causing it.

So, to combining n cues ($C_{1...n}$),

$$P(S|C_{1...n}) = \frac{P(C_{1...n}|S)P(S)}{P(C_{1...n})} \quad (\text{A.2})$$

which cannot be factorized. However, if we assume that the cues are independent, meaning that an error in one cue is unrelated to errors in any other cues, and that all priors are flat, i.e. no stimulus is more prevalent than others based on any individual cue or combination thereof, then

$$P(S|C_{1...n}) = \prod_{i=1}^n P_i(S|C_i) \quad (\text{A.3})$$

Taking logarithms of both sides,

$$\log P(S|C_{1...n}) = \sum_{i=1}^n \log P_i(S|C_i) \quad (\text{A.4})$$

Performing Taylor series expansions about the n cue stimulus estimators S_i^* ,

$$\log P(S|C_{1...n}) = \sum_{i=1}^n \log P_i(S_i^*|C_i) - \frac{1}{2} \sum_{i=1}^n w_i (S - S_i^*) + O\{(S - S_1^*)^3, \dots, (S - S_n^*)^3\} \quad (\text{A.5})$$

where weights $w_i = -\frac{d^2 \log P_i(S|C_i)}{dS^2}$. The first-order terms in the Taylor expansion vanish because S_i^* are extrema, and $\log P(S|C_{1...n}) \cong \sum_{i=1}^n \log P_i(S_i^*|C_i)$. Ignoring higher order terms, rearranging (A.5) therefore gives:

$$S = \frac{\sum_{i=1}^n w_i S_i^*}{\sum_{i=1}^n w_i} \quad (\text{A.6})$$

If the distributions are Gaussian, then the higher order terms in (A.5) vanish, and (A.6) is exact. In this case, weights are proportional to the inverse variances of the distributions, $\frac{1}{\sigma_i^2}$. This analysis is only valid if $S_1^* \approx S_2^* \approx \dots \approx S_n^*$. Therefore, ignoring differences between the cue estimates, the numerator in (A.6) becomes the sensitivity associated with the combined estimate (1) and (A.6) can be rewritten as (2).

Generally, in any real-world situation, assumptions are valid (or their validity can be proven) only to a certain degree. We have made several assumptions in this derivation, many of which are not clearly valid for the particular case of our stimuli and task. We will treat each of these assumptions in turn, describing exactly what it means in relation to the present study, and reasons why it is and is not valid.

A.1. Independence between cues

We manipulated envelope, patch and between-patches cues independently. However, it is not clear whether the visual system has independent mechanisms sensitive to each cue. In particular, although simple cells in V1 are tuned to phase, we are ignoring the fact that oriented filters between the patches will also be stimulated, or alternatively assuming that the visual system has a way of formulating independent estimates for orientation within and between the patches. Strictly, therefore, certain inferences from the cue-combination model are only valid with the caveat “if the visual system had independent mechanisms to estimate the three cues.” Additionally, others have argued that the interaction between first-order and second-order cues is precisely due to the lack of independent mechanisms (see Section 4). Our point here is rather to examine whether and to what extent the phenomenology of orientation perception accords with the weighted combination of independent cues, in the hope that the result of this enquiry will set bounds on possible mechanisms, without actually proposing any.

A.2. Flat priors

This assumption means that all orientations are equally probable, based on any combination of cues. This is clearly not true for within and between-patch cues, because only orientations near the within-patch orientation can be signaled by phase-shifts between patches. Additionally, there is a bias in nature towards horizontal orientations, and away from obliques, which is reflected by psychophysical variations in sensitivity, as well as differences in the number of cells tuned to those orientations (for review see Li, Peterson, & Freeman, 2003). However, within the range we tested ($\pm 5^\circ$ from horizontal) it seems reasonable to assume that priors are flat and independent.

A.3. Gaussian distributions

This means that the error associated with each cue, and their combination, is Gaussian-distributed. We already made this assumption when fitting the psychometric functions with cumulative normals using Probit, and such assumptions are common in psychophysics. However, orientation estimates based on phase-shift are bounded at $\pm 180^\circ$ phase angle and therefore at best only locally approximable by a Gaussian curve.

A.4. Similar estimators

This means that the orientations given by the three cues must be similar, compared with the variance of the cues, in order for the model to be valid. We introduced a cue conflict of upto 7° in the closest spacing of experiment 1, and 3.5° in the other experiments. Compare this with a threshold of 0.5° – 1.0° , and hence a variance of 0.25° – 1.00° . The cue conflict is in the range of between 3 and 10 times the variance. The model can be justified post hoc from the data, by noting that thresholds only increased slightly when cue-conflict was increased (grey lines in Fig. 2a, filled symbols in Fig. 4c), however this increase in thresholds cannot be captured by the model, and may have further ramifications concerning the validity of any other inferences.

References

- Akutsu, H., & Levi, D. M. (1998). Selective attention to specific location cues: the peak and center of a patch are equally accessible as location cues. *Perception*, 27, 1015–1023.
- Dakin, S. C., Williams, C. B., & Hess, R. F. (1999). The interaction of first- and second-order cues to orientation. *Vision Research*, 39, 2867–2884.
- Field, D. J., Hayes, A., & Hess, R. F. (1993). Contour integration by the human visual system: evidence for a local association field. *Vision Research*, 33, 173–193.

- Finney, D. J. (1971). *Probit analysis* (3rd ed.). Cambridge: Cambridge University Press.
- Fraser, J. (1908). A new visual illusion of direction. *British Journal of Psychology*, 2, 307–320.
- Hansel, D., & van Vreeswijk, C. (2002). How noise contributes to contrast invariance of orientation tuning in cat visual cortex. *Journal of Neuroscience*, 15, 5118–5128.
- Hillis, J. M., Ernst, M. O., Banks, M. S., & Landy, M. S. (2002). Combining sensory information: mandatory fusion within, but not between, senses. *Science*, 298, 1627–1630.
- Kersten, D., & Schrater, P. R. (2002). Pattern inference theory: a probabilistic approach to vision. In R. Mausfeld & D. Heyer (Eds.), *Perception and the physical world* (pp. 191–228). Chichester: John Wiley & Sons Ltd.
- Levi, D. M., Wing-Hong Li, R., & Klein, S. A. (2003). Phase capture in the perception of interpolated shape: cue combination and the influence function. *Vision Research*, 43, 2233–2243.
- Li, B., Peterson, M. R., & Freeman, R. D. (2003). Oblique effect: a neural basis in the visual cortex. *Journal of Neurophysiology*, 90, 204–217.
- Mareschal, I., & Baker, C. L. Jr., (1998). A cortical locus for the processing of contrast-defined contours. *Nature Neuroscience*, 1, 150–154.
- Morgan, M. J., & Baldassi, S. (1997). How the visual system encodes the orientation of a texture and why it makes mistakes. *Current Biology*, 7, 999–1002.
- Morgan, M. J., Mason, A. J. S., & Baldassi, S. (2000). Are there separate first-order and second-order mechanisms for orientation discrimination? *Vision Research*, 40, 1751–1763.
- Nothdurft, H.-C., Gallant, J. L., & Van Essen, D. C. (1999). Response modulation by texture surround in primate area V1: correlates of “popout” under anesthesia. *Visual Neuroscience*, 16, 15–34.
- Peterhans, E., & von der Heydt, R. (1993). Functional organization of area V2 in the alert macaque. *European Journal of Neuroscience*, 1, 509–524.
- Popple, A. V., & Levi, D. M. (2000a). A new illusion demonstrates long-range processing. *Vision Research*, 40, 2545–2549.
- Popple, A. V., & Levi, D. M. (2000b). Amblyopes see true alignment where normal observers see illusory tilt. *Proceedings of the National Academy of Sciences of the United States of America*, 97, 11667–11672.
- Popple, A. V., & Sagi, D. (2000). A Fraser illusion without local cues? *Vision Research*, 40, 873–878.
- Skillen, J., Whitaker, D., Popple, A. V., & McGraw, P. V. (2002). The importance of spatial scale in determining illusions of orientation. *Vision Research*, 42, 2447–2455.
- Yuille, A. L., & Bulthoff, H. H. (1995). Bayesian decision theory and psychophysics. In D. C. Knill & W. Richards (Eds.), *Bayesian perspectives on visual perception*. Cambridge: Cambridge University Press.